

Technical University of Denmark



Multi-fidelity wake modelling based on Co-Kriging method

Wang, Y. M.; Réthoré, Pierre-Elouan; van der Laan, Paul; Murcia Leon, Juan Pablo; Liu, Y. Q.; Li, L.

Published in:
Journal of Physics: Conference Series (Online)

Link to article, DOI:
[10.1088/1742-6596/753/3/032065](https://doi.org/10.1088/1742-6596/753/3/032065)

Publication date:
2016

Document Version
Publisher's PDF, also known as Version of record

[Link back to DTU Orbit](#)

Citation (APA):
Wang, Y. M., Réthoré, P-E., van der Laan, P., Murcia Leon, J. P., Liu, Y. Q., & Li, L. (2016). Multi-fidelity wake modelling based on Co-Kriging method. Journal of Physics: Conference Series (Online), 753(3), [032065]. DOI: 10.1088/1742-6596/753/3/032065

DTU Library

Technical Information Center of Denmark

General rights

Copyright and moral rights for the publications made accessible in the public portal are retained by the authors and/or other copyright owners and it is a condition of accessing publications that users recognise and abide by the legal requirements associated with these rights.

- Users may download and print one copy of any publication from the public portal for the purpose of private study or research.
- You may not further distribute the material or use it for any profit-making activity or commercial gain
- You may freely distribute the URL identifying the publication in the public portal

If you believe that this document breaches copyright please contact us providing details, and we will remove access to the work immediately and investigate your claim.

Multi-fidelity wake modelling based on Co-Kriging method

This content has been downloaded from IOPscience. Please scroll down to see the full text.

2016 J. Phys.: Conf. Ser. 753 032065

(<http://iopscience.iop.org/1742-6596/753/3/032065>)

View [the table of contents for this issue](#), or go to the [journal homepage](#) for more

Download details:

IP Address: 192.38.90.17

This content was downloaded on 08/12/2016 at 09:39

Please note that [terms and conditions apply](#).

You may also be interested in:

[Multi-fidelity design optimization of Francis turbine runner blades](#)

S Bahrami, C Tribes, S von Fellenberg et al.

[Resilient algorithms for reconstructing and simulating gappy flow fields in CFD](#)

Seungjoon Lee, Ioannis G Kevrekidis and George Em Karniadakis

Multi-fidelity wake modelling based on Co-Kriging method

Y M Wang¹, P-E Réthoré², M P van der Laan², J P Murcia Leon², Y Q Liu¹ and L Li¹

¹ State Key Laboratory of Alternate Electrical Power System with Renewable Energy Sources, North China Electric Power University, Beijing 102206, China.

² Department of Wind Energy, Technical University of Denmark, Risø campus, 4000 Roskilde, Denmark.

Email: wym0504@126.com

Abstract. The article presents an approach to combine wake models of multiple levels of fidelity, which is capable of giving accurate predictions with only a small number of high fidelity samples. The G. C. Larsen and $k-\varepsilon-f_p$ based RANS models are adopted as ensemble members of low fidelity and high fidelity models, respectively. Both the univariate and multivariate based surrogate models are established by taking the local wind speed and wind direction as variables of the wind farm power efficiency function. Various multi-fidelity surrogate models are compared and different sampling schemes are discussed. The analysis shows that the multi-fidelity wake models could tremendously reduce the high fidelity model evaluations needed in building an accurate surrogate.

1. Introduction

Due to the up-scaling of wind farms, wind turbine wake simulations become more challenging, and more and more high fidelity wake models are developed by different institutions. The design of wind farms and the calculation of annual energy production (AEP), taking uncertainty into account, always require a large number of wake model evaluations. Compared to the simple and fast engineering models, the wake simulations based on computational fluid dynamics (CFD) methods often give more information and yield better calculation results. High fidelity wake models are impractical for the calculation of the AEP and wind farm layout optimization due to the need of large computational resources. An efficient way to reduce the required computational resources for accurate AEP calculations, is to build a surrogate model of the high fidelity wake model.

The concept of a surrogate model is to replace a complex wake simulation method by establishing the approximated model of the target function (wind farm efficiency or AEP), such that the number of high fidelity model evaluations needed to calculate the AEP is reduced. A large number of statistical methods can be used to build the surrogate model, such as Neural Network, Radial Basis Function, Kriging and Response Surface method [1, 2, 3]. For the efficient AEP calculation, the Polynomial Chaos technique [4] has been used to build the surrogate of a stationary wind farm flow model. Apart from the above fitting methods, the multi-fidelity method [5] has also gained a lot of attention. The multi-fidelity method combines accurate and often expensive models with models that are faster to run but also produce results of low accuracy. By taking a large amount of low fidelity model results and only a few high fidelity model results to increase the accuracy of the surrogate model, the multi-fidelity method can significantly reduce the computational cost.



As for the AEP calculation, a large amount of model evaluations is needed to build an accurate surrogate. Thus, how to reduce the computational resources required by the surrogate model is still not clear. Based on the approach of Loic Le Gratiet [6], the presented article makes full use of the effectiveness of low fidelity wake models and the accuracy of high fidelity wake models, and proposes a framework for multi-fidelity wake modelling. The G.C. Larsen model [7] and a RANS model using the $k-\varepsilon-f_p$ turbulence model [8] are adopted as the low fidelity and the high fidelity ensemble members, respectively. Both wind speeds and wind directions are taken as input variables, and different sampling strategies are investigated to build the surrogate model. The objective of the present work is to demonstrate how a multi-fidelity surrogate wake model can be used to obtain more accurate and faster wind power and energy production calculations. The Lillgrund wind farm is used as a test case to analyze and validate the effectiveness of this multi-fidelity model.

2. Methodology

This section describes the adopted methodologies, including the wake models used for aggregation, the Quantities of Interest that need to be surrogated, the Kriging and Co-Kriging interpolation techniques, and the sampling methods used for choosing the high fidelity samples.

2.1. The wake models for aggregation

One of the key factors to obtain an accurate multi-fidelity surrogate model is to have a good low fidelity model which could give well predictions of high fidelity trends. Two different wake models developed at Technical University of Denmark (DTU) are respectively taken as the low fidelity (LF) and high fidelity (HF) model, which are the G. C. Larsen model and the $k-\varepsilon-f_p$ based RANS model. The principles and relative equations about the two models have been fully described by Gunner C. Larsen [7] and van der Laan et al. [8], and a brief overview about the two models is presented here.

2.1.1. G. C. Larsen model. The G. C. Larsen model (GCL) is a semi-analytical wake model used for the computation of stationary wind farm flow fields, and it is a very fast semi-empirical engineering model. GCL considers wakes as linear perturbations on the non-uniform ambient mean wind field, although the non-linear terms are included in the modelling of the individual stationary wake flow fields. The simulations of each individual wake contribution are based on an analytical solution of the thin shear layer approximation of the Navier-Stokes equations. The wake flow fields are assumed rotationally symmetric, and the rotor inflow fields are consistently assumed as uniform. The implementation of the GCL model used in this paper is accessible in the open source wind farm flow model library FUSED-Wake (<https://github.com/DTUWindEnergy/FUSED-Wake>), the power curve and coefficient curve used to calculate the total output power of the whole wind farm are publicly available from the wind turbine manufacturer.

2.1.2. $k-\varepsilon-f_p$ based RANS model. The RANS equations are solved by EllipSys3D [9, 10], the in-house flow solver of DTU Wind Energy. The turbulence is modelled by the $k-\varepsilon-f_p$ model, a modified $k-\varepsilon$ model [11], which is able to predict with more accuracy the near wake velocity deficit of actuator disks (AD) [12] situated in an atmospheric boundary layer. The ADs are loaded by thrust force distributions which are dynamically scaled by a thrust coefficient C_T^* that is a function of the local AD velocity averaged over the AD, U_{AD} [13]. For a given case, the $C_T^*-U_{AD}$ curve is obtained from a parametric run of single wind turbine simulations for free stream velocities of 4-25 m/s, where the standard thrust coefficient of the manufacturer is set. The rotational force is neglected because its effect on the power deficit is small [8]. The parametric run of single wind turbine simulations also provides a $P-U_{AD}$ curve that is used to post process the power of each AD in the wind farm simulations. Neutral (logarithmic) inflow conditions are set at the inlet and the bottom boundary is modelled as a rough wall. A turbulence intensity at hub height (Ti_H) of 4.8% is set by the roughness height z_0 and z_H [11].

$$Ti_H = \frac{\sqrt{2/3k}}{U_H} = \frac{\kappa \sqrt{2/3}}{\ln(z_H/z_0) \sqrt{C_\mu}} \quad (1)$$

Where k is the turbulent kinetic energy, U_H is the stream wise velocity at the hub height velocity, κ is the von Karman constant and C_μ is the eddy-viscosity coefficient.

2.2. Quantities of Interest

The normalized wind farm efficiency (NE) and the expected wind farm efficiency (EE) are taken as the Quantities of Interest (QoI). The NE is defined as the total output power normalized by the power of a single wind turbine without wake effects and the number of wind turbines. Since the performance of a wind farm is always evaluated by the expected energy production over years, and the annual energy production (AEP) is the most common evaluation index during the process of wind farm design and evaluation, the expected wind farm efficiency is also computed as a surrogate target. The EE represents a weighted contribution of the NE to the AEP, which is defined as the NE multiplied by the joint probability density distribution (PDF) of the corresponding averaged wind speed u and averaged wind direction θ .

$$NE(u, \theta) = \frac{P(u, \theta)}{pc(u)N_{wt}} \quad (2)$$

$$EE(u, \theta) = NE(u, \theta)PDF(u, \theta) \quad (3)$$

$$AEP = 8760 N_{wt} \int_0^{2\pi} \int_0^\infty EE(u, \theta) pc(u) du d\theta \quad (4)$$

Where $P(u, \theta)$ is the total power output of the wind farm for a given wind speed and wind direction, $pc(u)$ is the power output of a single wind turbine without wake effects for a given wind speed, N_{wt} is the number of wind turbines, $PDF(u, \theta)$ is the joint PDF of wind speed and wind direction.

2.3. Interpolation and surrogate method

Kriging and Co-Kriging based surrogate wake models are established in this paper. Based on the work of Sacks et al. [14], Kennedy and O'Hagan [15], Rasmussen C. E. [16] and Forrester et al. [5], a brief theoretical description of Kriging and Co-Kriging is provided here. The codes are implemented using the package scikit-learn as basis and based on the open-source OpenMDAO platform [17].

2.3.1. Kriging method. Kriging is a stochastic interpolation technique which assumes that the real model output is a realization of a Gaussian process, and could be expressed as follows:

$$y(x) = \mu(x) + z(x) \quad (5)$$

Where $\mu(x)$ is the mean value of the Gaussian process and $z(x)$ is a zero-mean Gaussian process with a fully stationary covariance function:

$$C(x, x') = \sigma^2 R(x, x' | \theta) \quad (6)$$

Where σ^2 is the variance, R is the correlation function which depends only on the absolute relative distance between each sample and θ gathers the hyper parameters of R . There is a wide range of kernels that could be chosen as the correlation function R , such as squared exponential kernel, Gaussian kernel and Mat érn kernel. For the universal Kriging case, the mean value is calculated as a combination of unknown linear regression coefficients β_j and a set of preselected basis functions $f_j(x)$.

$$\mu(x) = \sum_{j=0}^m \beta_j f_j(x) \quad (j=1, 2, \dots, m) \quad (7)$$

For a given case, a design of experiments is formed as $X=[x_1, x_2, \dots, x_n]$, and a corresponding set of model simulations are gathered as $Y=[M(x_1), M(x_2), \dots, M(x_n)]$. Then based on the best linear unbiased prediction (BLUP), the Kriging predicted response at a new unknown point $x^* \in D_x$ is a Gaussian variable $\hat{Y}(x^*)$ with mean $\mu_{\hat{Y}}$ and variance $\sigma_{\hat{Y}}^2$, which are defined as:

$$\mu_{\hat{Y}}(x^*) = E[\hat{Y}(x^*) | M(x^{(i)})] = f^T \hat{\beta} + r^T R^{-1} (Y - F\hat{\beta}) \quad (8)$$

$$\sigma_{\hat{Y}}^2(x^*) = \text{Var}[\hat{Y}(x^*) | M(x^{(i)})] = \sigma_Y^2 (1 - r^T R^{-1} r + u^T (F^T R^{-1} F)^{-1} u) \quad (9)$$

where the optimal Kriging variance σ_Y^2 and the generalized least square regression weights $\hat{\beta}$ are given by:

$$\sigma_Y^2 = \frac{(Y - F\hat{\beta})^T R^{-1} (Y - F\hat{\beta})}{n} \quad (10)$$

$$\hat{\beta} = (F^T R^{-1} F)^{-1} F^T R^{-1} Y \quad (11)$$

And u , F , r are given by $u = F^T R^{-1} r - f$, $F = [f_j(x^{(i)})]$ and $r = [r_1, r_2, \dots, r_n]^T$, where $r_i = R(x^* - x^i) | \theta$ ($i=1, 2, \dots, n$).

2.3.2. Co-Kriging method. Co-Kriging is an extension of Kriging, it has the same interpolation principle as Kriging, but with taking the results of low fidelity as the prior. If the high fidelity model is M_e and the low fidelity model is M_c , and then the Co-Kriging model can be described as:

$$\mu_{\hat{Y}}^{(e)} = \rho \mu_{\hat{Y}}^{(c)} + r^T R'^{-1} (Y - F\hat{\beta}') \quad (12)$$

Where ρ is a scaling factor that has a similar description as equation (11), $\mu_{\hat{Y}}^{(c)}$ is the trend in the Kriging of the low fidelity data, and $r^T R'^{-1} (Y - F\hat{\beta}')$ depends only on high fidelity samples.

2.4. Sampling methods

The surrogate model should not only be capable of fitting the sample data, but should also be able to predict the value of non-sample points in the design space. The sample size and scheme will have an impact on both the accuracy of the surrogate and the computational resources needed by the surrogate.

A common principle for sampling methods is that the samples have to cover the whole design space and be able to represent the characters of the whole design. Based on that principle, three different sampling schemes, namely uniform sampling, extreme point sampling and random sampling, are used to determine the location of high fidelity samples. The uniform sampling is to sample uniformly in both the wind speed and wind direction dimensions. The extreme point sampling is conducted for every given wind speed, and the local extreme points of the low fidelity results are taken as the samples in wind direction dimension. The random sampling is conducted by using Latin Hypercube Sampling (LHS) method. LHS [18] is a statistical method for generating a sample of plausible collections of parameter values from a multi-dimensional distribution. The selected samples of LHS could be uniformly distributed in the whole design space. Assuming there are m design variables, and the sample size is n . The LHS method usually divides the variation range of every variable into n intervals, and the intervals would be equal if the design is even enough, and finally the design space will be divided into m^n sub-regions by LHS. One of the advantages of LHS appears when the output is dominated by only a few of the components of inputs. LHS ensures that each of those components is represented in a fully stratified manner, no matter which components might turn out to be important.

3. Case Analysis

The Lillgrund wind farm is used to assess the established surrogate models, a wide range of wind speeds and wind directions are considered as input wind conditions to carry on both univariate and multivariate wake modelling.

3.1. Wind farm description

Lillgrund is an offshore wind farm, located at the southern coast of Sweden. It consists of 48 Siemens SWT93-2.3 MW wind turbines, and the layout as well as the power and thrust coefficient curves are show in Figure 1. The PDF of different wind conditions is taken as the function of both wind speed and wind direction. According to wind turbine power curve, the wind speeds that contribute to the AEP range from the cut in wind speed (4 m/s) to the cut out wind speed (25 m/s). The investigated wind direction covers the whole wind rose (from 0° to 360°, 0° represents north wind), which is uniformly divided into 12 sectors and the wind directions within each sector are assumed to have the same probability. The frequency of each wind direction sector and the Weibull distributions of wind speed within each sector could be obtained from the statistical data of the wind farm, and based on that, the PDF of every possible wind condition could be computed, which is shown in Figure 2.

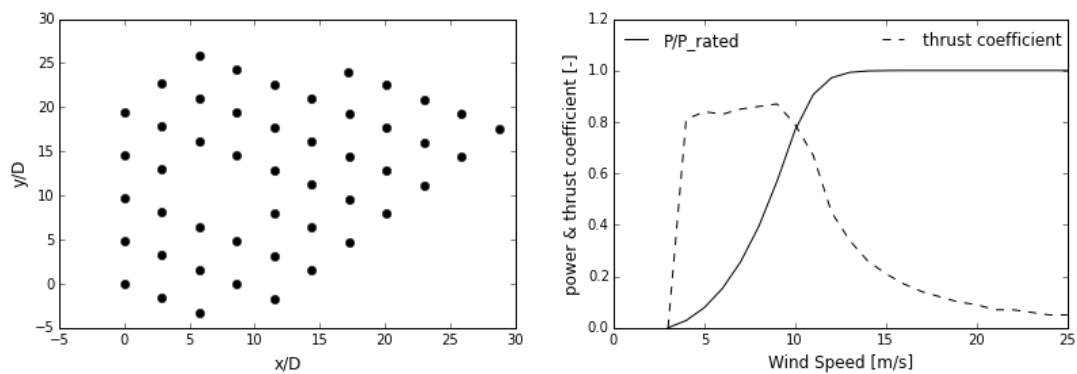


Figure 1. Layout (left) and power and thrust coefficient curves (right) for wind turbines.

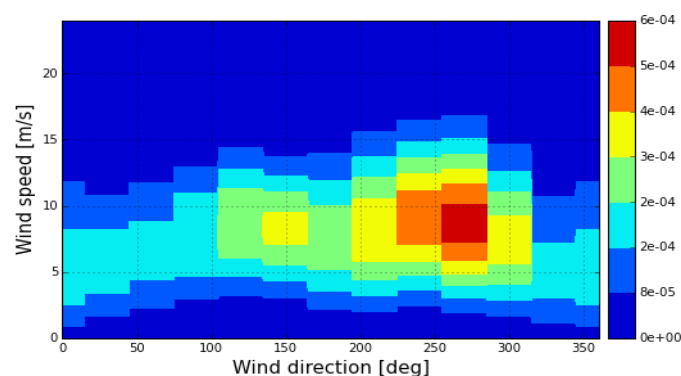


Figure 2. PDF map for all wind speeds and wind directions.

For Lillgrund wind farm, the GCL model and RANS model are taken as the low fidelity and high fidelity models, respectively. For a single flow case, the computation costs of GCL and RANS models are explained in Table 1. Since the value of thrust coefficient below the cut in wind speed is still unclear, both of the two wake models are evaluated from 5 m/s to 24 m/s (every 1 m/s) for the full wind rose. For each given wind speed, the low fidelity GCL model is evaluated every 1°, and the high fidelity RANS model is evaluated every 3°. Based on all those model evaluation results, the relationship between the input wind conditions and output efficiencies of each model can be built by using cubic spline function. Then, the interpolated results are assumed as the true model outputs. The

mean relative error (MRE) is calculated to evaluate the prediction performance of the surrogate Kriging and Co-Kriging models.

$$MRE = \frac{1}{N} \sum_{i=1}^N \frac{|y_{pred} - y|}{y} \quad (13)$$

Where N is the test points number, y_{pred} is the predicted efficiency of surrogate model and y is the true efficiency value of every test sample.

Table 1. The costs of GCL model and RANS model for a single flow case (Lillgrund case).

	Low Fidelity	High Fidelity
Wake model	GCL model	$k-\epsilon-f_P$ based RANS model
Time	20 milliseconds	30 minutes
CPU	1 core of 2.66GHz	140 cores of 2.8GHz

3.2. Univariate surrogate model

3.2.1. Surrogate with different variables. Both wind direction and wind speed are key components for AEP calculation. For univariate modelling, the wind farm efficiency is separately computed as the function of wind speed for a fixed wind direction and the function of wind direction for a fixed wind speed. The 9 m/s and 270° cases are separately taken as a fixed wind speed and wind direction because they have a high contributions to final AEP.

Based on the wake model evaluations, the normalized wind farm efficiency curves for 9 m/s and 270° can be obtained, and the expected wind farm efficiency can also be calculated. Figure 3 shows the comparison of different efficiency curves together with the PDF with respect to wind direction and wind speed separately. Figure 3 illustrates that the efficiency curves calculated by low fidelity GCL model and high fidelity RANS model have similar variation trends for both variables. The expected efficiency curve of 9 m/s shows discontinuities because of the discontinuous PDF curve of wind direction.

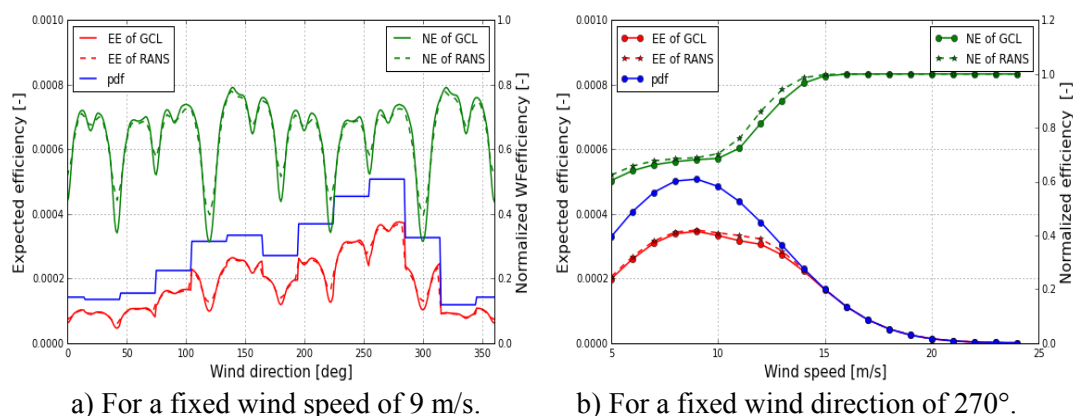


Figure 3. The normalized and expected efficiency curves giving respect to different variables.

The Kriging of high fidelity RANS model is established based only on RANS data. Figure 4 shows the error convergence curves for both the normalized efficiency and expected efficiency. For the study of sample size on each variable, a set of uniformly distributed 5 points covering the whole wind speed or wind direction range are selected as a start. To reduce the Kriging error, a new evaluation point

which gives the maximum predicted uncertainty will be added in the next run. As we can see from Figure 4, due to the discontinuity of PDF curve, more training points are needed for the expected efficiency to get the same accuracy as normalized efficiency. For the surrogate of normalized efficiency, it takes more than 50 training points to achieve an error of 10^{-2} for the wind direction variable, while only 7 points are needed when the wind speed is taken as the variable. This shows that the smoother the target function is, the fewer samples are needed by the Kriging method in order to get an accurate high fidelity surrogate.

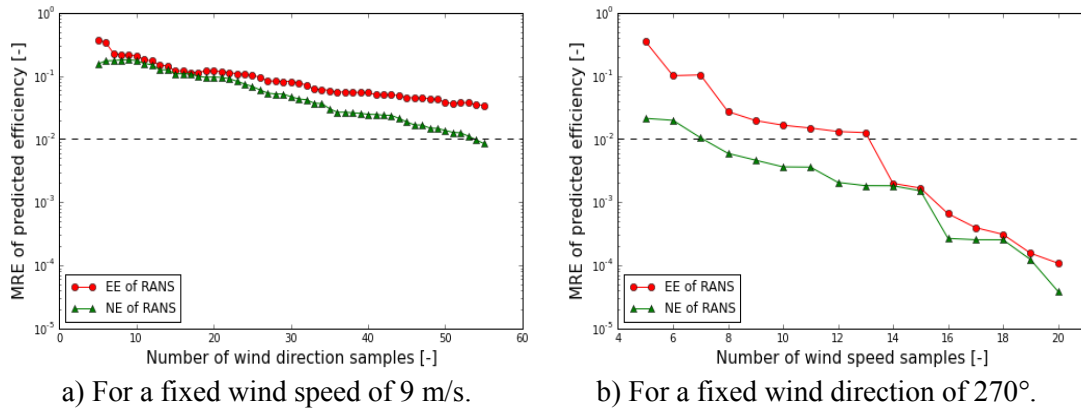


Figure 4. Error curves of Kriging prediction for different variables giving respect to sample size.

3.2.2. *Surrogate with wind direction.* Since it is more difficult to get an accurate surrogate of wind farm efficiency as the function of wind direction, here three different sampling schemes are used to surrogate with wind direction for a fixed wind speed of 9 m/s. A wide range of uniformly spaced points, LHS based random points and extreme points are taken respectively as the high fidelity samples, 361 uniformly spaced points are taken as the low fidelity samples. Figure 5 shows the error convergence curves of the Kriging and Co-Kriging models with respect to the number of high fidelity wind direction samples. The surrogate object is the normalized wind farm efficiency.

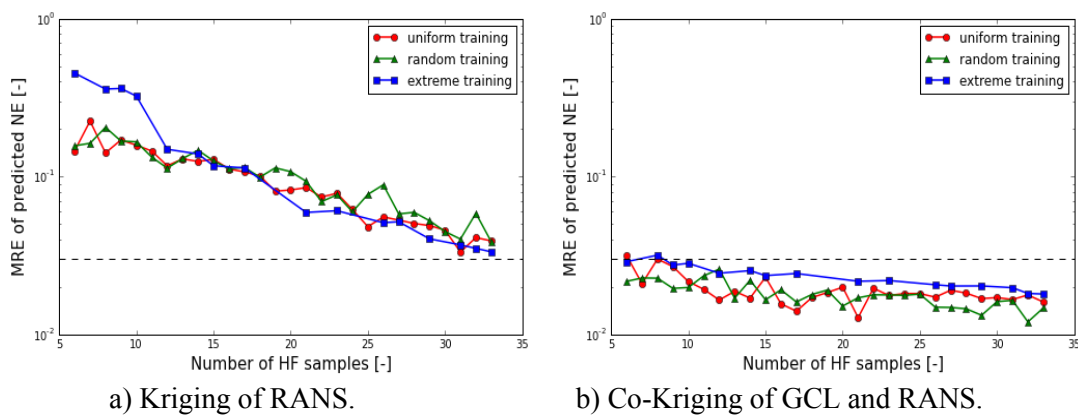
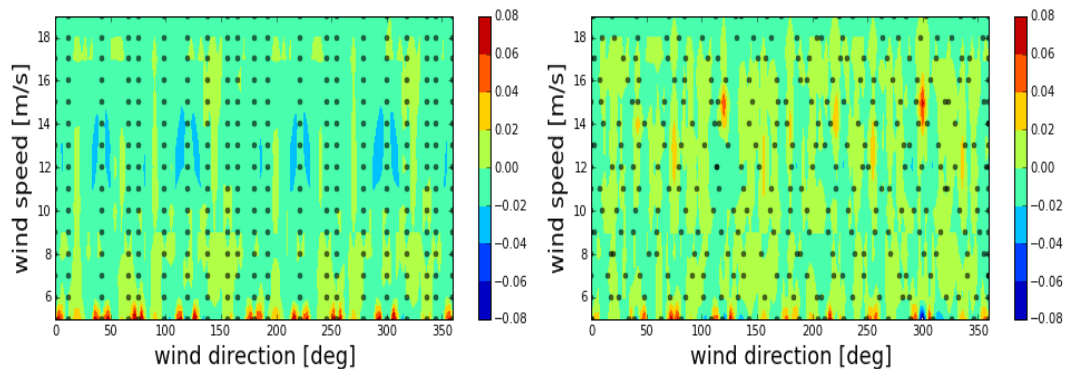


Figure 5. Error convergence curves of different sampling methods.

Figure 5 shows that, with the same number of high fidelity samples, the Co-Kriging model which takes low fidelity results as the prior information gives more accurate predictions than Kriging model which uses only high fidelity data. For these three sampling strategies, random and uniform sampling show almost the same performance, while the extreme points sampling gives a lower error for the Kriging model and a higher error for the Co-Kriging model. When 33 high fidelity samples are used, the three sampling schemes have a similar error, in the order of 10^{-2} .

3.2.3. *Surrogate between neighboring wind speed.* Based on the analysis of a large amount of low fidelity evaluations, the wind farm efficiency as a function of wind direction has similar variation trends between neighboring wind speeds. It means that the surrogate output of one wind speed could also be taken as a low fidelity prior input for the surrogate of neighboring wind speeds.

The normalized wind farm efficiency increases with the increase of wind speed, but cannot be higher than one due to its definition. Since the stochastic Kriging cannot take that into consideration, a logistic function is needed to transfer the wind farm efficiency from the space of zero to one to the space of infinity, and then an inverse logistic function is used to transfer the Kriging prediction back to the real predicted efficiency.



a) Taking extreme points as HF sample. b) Taking random points as HF sample.

Figure 6. Error of Co-Kriging predictions by taking the data of 9 m/s as a prior. Black points represent HF samples.

The Co-Kriging surrogate of 9 m/s is taken as the initial prior, i.e. it is taken as the low fidelity model for the surrogate of 8 m/s and 10 m/s. Then all the wind speeds are divided into two groups, where one is higher than 9 m/s, and the other is lower than 9 m/s. As explained above, the surrogate results of 10 m/s and higher wind speeds are respectively taken as the prior low fidelity of their neighboring high wind speed, and the surrogate of 8 m/s and lower wind speeds are respectively taken as the prior of their neighboring low wind speed. 21 HF samples and 121 LF samples are used for the surrogate of every target wind speed. For HF samples, both the extreme and random sampling schemes are discussed. With the tuning of logistic and inverse logistic function, the error map of the whole prediction space can be obtained as shown in Figure 6. For either of the two sampling methods, the surrogate of low wind speed (5 m/s) gives high errors. In addition, it is also a little difficult to give very accurate predictions for the wind speeds (12-15 m/s) around rated wind speed.

3.3. *Multivariate surrogate model*

The normalized wind farm efficiency is taken as the function of both wind speed and wind direction. Based on LHS method, some sets of random HF samples are selected to build the Kriging and Co-Kriging surrogate models. Figure 7 shows the error convergence curves of the Kriging and Co-Kriging models with respect to the number of high fidelity samples. Figure 7 also presents the similar results as univariate surrogate, i.e. the Co-Kriging model can produce more accurate predictions than the Kriging model by using the same number of high fidelity samples. In order to illustrate the different predictions of different surrogate models, 300 random samples covering the whole design space are selected as the high fidelity sample to build the Kriging surrogate of the RANS results. In addition, 70 random points which cover the whole design space are also selected as the high fidelity samples of Co-Kriging model, where 2420 uniformly spaced low fidelity samples are used as the prior information. The predicted errors of different surrogate models are shown in Figure 8.

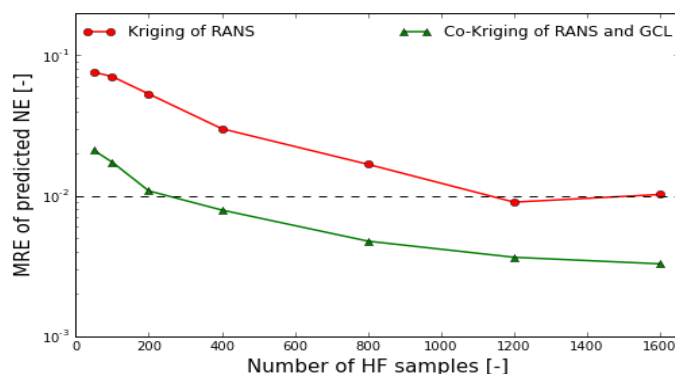


Figure 7. Error convergence curves of different surrogate models

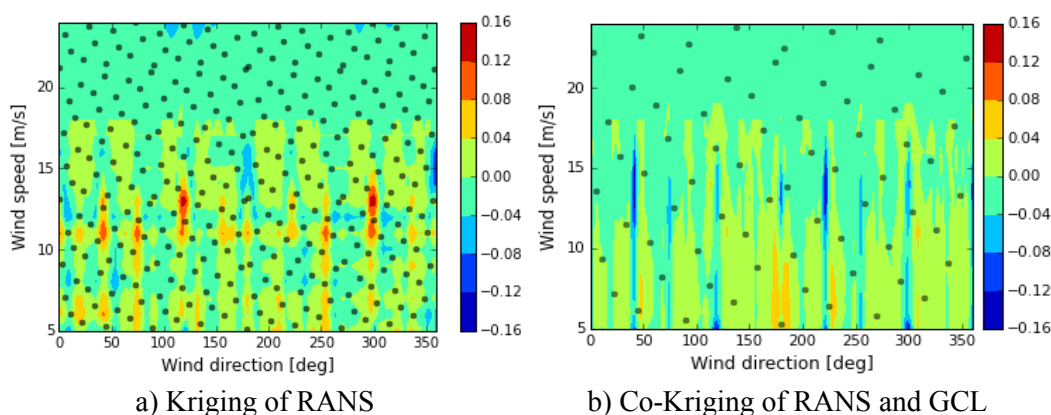


Figure 8. The error maps of different surrogate models. Black points represent HF samples.

As illustrated in Figure 8, by taking a large number of low fidelity results as a prior in the Co-Kriging method, it is much easier to capture the variation trends of the target function, compared to using only a small set of high fidelity model results in the Kriging method. In addition, the Co-Kriging method reduces the required number of high fidelity model evaluations. Thus, by using multi-fidelity wake modelling methods, the reduction of the computation resources would be very promising.

4. Discussion

The advanced interpolation techniques, Kriging and Co-Kriging are adopted to build the surrogate of a high fidelity RANS model, and both the univariate and multivariate modelling techniques are explored. According to the case analysis and relevant results, the discussion and the potential future investigations could be given as follows.

1) For univariate surrogate, it is much easier to build a surrogate model based on wind speed compared to wind direction, because the wind farm efficiency is a smoother function of wind speed than wind direction. The efficiency curves produced by the models of various fidelities take on similar variation trends, and a larger model difference can be seen for the wind directions in which more wind turbines are aligned. In order to have a clear conclusion about the wind conditions where extra high fidelity model evaluations are needed, the wind farms with different layouts should also be studied.

2) For the univariate surrogate with wind direction, given the same high fidelity samples, the Co-Kriging model can produce more accurate predictions than the Kriging model. When considering about the error convergence curves of different sampling methods, uniformly and randomly samplings have almost the same performance, especially when many samples are used. However, the extreme point sampling is different, and it could give valuable information needed by Kriging. Whereas the information needed by Co-Kriging is how to improve the low fidelity results in an overall way, which means using only the extreme points sampling may overcorrect the whole space and make high errors.

3) In the shown test case, the wind direction sector is a bin of 30° , and the wind direction within each sector is assumed to have the same probability, which is too coarse for this analysis. The coarse wind direction bins also produce abruptly changing curves of expected efficiency, which made it difficult to obtain an accurate surrogate model. In future research, a continuous PDF of wind direction should be calculated based on the raw measurement data of test site. As a result, a more smooth expected efficiency function will be obtained, which can directly be used as the surrogate object.

4) For the univariate surrogate between neighboring wind speed, the random sampling for different single wind speed performs better than using the same extreme points for every wind speed. Especially for the extension to multi-dimension space, it is better to have the samples which are able to cover the whole design space or at least all the meaningful space. If the surrogate is served for a specific application, such as AEP calculation, then a sample design could be made based on the distribution of input variables, i.e. give higher weights to more meaningful area so that to increase the efficiency and reduce the costs of the surrogate.

5) For the surrogate with two-dimensional inputs, the wind farm efficiency is taken as the function of both wind speed and wind direction. To achieve an MRE of 1% for the whole validation area, Kriging needs 1200 HF samples, while Co-Kriging needs only 200 HF samples. Besides, the difference between high fidelity and low fidelity data could replace the high fidelity data and be the input of Co-Kriging model, which is another significant parameter that deserves more research.

5. Conclusions

The G. C. Larsen model and $k-\varepsilon-f_p$ based RANS model are taken as low fidelity and high fidelity wake models, respectively. Based on Kriging and Co-Kriging method, both the univariate and multivariate modelling techniques are discussed, and the following conclusions can be drawn: 1) For univariate surrogate, the wind farm efficiency with respect to wind speed is easier to surrogate than with respect to wind direction, which means fewer samples are need to get an accurate surrogate for wind farm efficiency as function of wind speed than as function of wind direction. 2) The Co-Kriging model that uses data from models of multiple levels of fidelity produces better predictions than the Kriging model which takes only the high fidelity model as input. 3) Compared with other sampling schemes, the extreme points sampling produces a lower Kriging error, but a higher Co-Kriging error. A combination of different sampling methods could be considered in the future work. 4) Since the wind power efficiency curves for various wind speeds share similar variation trends, the surrogate model for a single wind speed could be taken as a low fidelity prior knowledge for the surrogate of neighboring wind speeds, using samples distributed over the whole space would help to produce a more accurate prediction. 5) The Co-Kriging with two-dimensional input has lower errors than Kriging, and could tremendously reduce the model evaluations needed by high fidelity wake model.

Acknowledgements

This work is supported by the National Natural Science Foundation of China (Grant No. 51376062). The first author is currently doing joint-educated PhD program in Technical University of Denmark, sponsored by China Scholarship Council. Also thanks to the International Collaborative Energy Technology R&D Program of the Korea Institute of Energy Technology Evaluation and Planning (KETEP), granted financial resource from the Ministry of Trade, Industry & Energy, Republic of Korea (No. 20138520021140).

References

- [1] Forrester A I J and Keane A J 2009 Recent advances in surrogate-based optimization *Prog. Aerosp. Sci.* **45** 50–79
- [2] Knill D L, Giunta A A, Baker C A, Grossman B, Mason W H, Haftka R T and Watson L T 1999 Response surface models combining linear and Euler aerodynamics for supersonic transport design *J. Aircr.* **36** 75–86
- [3] Mehmani A, Tong W, Chowdhury S and Messac A 2015 Surrogate-based Particle Swarm

Optimization for Large-scale Wind Farm Layout Design 1–6

- [4] Murcia J P, Réthoré P E, Natarajan A and Sørensen J D 2015 How many model evaluations are required to predict the AEP of a wind power plant? *J. Phys. Conf. Ser.* **625** 012030
- [5] Forrester A I J, Sobester A and Keane A J 2007 Multi-fidelity optimization via surrogate modelling *Proc. R. Soc. A Math. Phys. Eng. Sci.* **463** 3251–69
- [6] Le Gratiet L 2013 *Multi-fidelity Gaussian process regression for computer experiments* (Paris-Diderot)
- [7] Larsen G C 2009 *A simple stationary semi-analytical wake model* Technical report, risø-r-1713(en) Risø-DTU
- [8] van der Laan M P, Sørensen N N, Réthoré P-E, Mann J, Kelly M C, Troldborg N, Hansen K S and Murcia J P 2015 *Wind Energy* **17**, 2065
- [9] Sørensen N N 1994 General purpose flow solver applied to flow over hills Ph.D. thesis DTU
- [10] Michelsen J A 1992 Basis3d - a platform for development of multiblock PDE solvers. *Tech. rep.* DTU
- [11] van der Laan M P, Sørensen N N, Réthoré P E, Mann J, Kelly M C, Troldborg N, Schepers J G and Macheaux E 2015 *Wind Energy* **18** 889
- [12] Mikkelsen R 2003 Actuator Disc Methods Applied to Wind Turbines *PhD thesis, Tech. Univ. Denmark, Mek*
- [13] van der Laan M P, Sørensen N N, Réthoré P E, Mann J, Kelly M C and Troldborg N 2015 *Wind Energy* **18**, 2223
- [14] Jerome Sacks, Williams J. Welch, Toby J. Mitchell H P W 1989 Design and Analysis of Computer Experiments *Stat. Sci.* **4** 409–23
- [15] Kennedy M C and O’Hagan A 2000 Predicting the output from a complex computer code when fast approximations are available *Biometrika* **87** 1–13
- [16] Rasmussen C E, Williams C K 2006 *Gaussian processes for machine learning* (MIT Press)
- [17] Vauclin R, Dubourg V, Lafage R Multifidelity-cokriging *GitHub repository* https://github.com/OpenMDAO/OpenMDAO/tree/master/openmdao/surrogate_models
- [18] McKay M D, Beckman R J and Conover W J 1979 Comparison of Three Methods for Selecting Values of Input Variables in the Analysis of Output from a Computer Code *Technometrics* **21** 239–45